Original Article

Dosimetric Comparison between Single-energy Computed Tomography and Dual-energy Computed Tomography Relative to Stopping Power Estimation in Proton Therapy

Thamonwan Chirdchid[1]*, Sirinya Ruangchan[2,3]*, Taweap Sanghangthum[1,2,4]

[1]Department of Radiology, Faculty of Medicine, Chulalongkorn University, [2]Her Royal Highness Princess Maha Chakri Sirindhorn Proton Center, [3]Department of Radiology, Division of Radiation Oncology, King Chulalongkorn Memorial Hospital, Thai Red Cross Society, [4]Department of Radiology, Division of Radiation Oncology, Faculty of Medicine, Chulalongkorn University, Bangkok, Thailand

*These authors have contributed equally to this work

Abstract

Purpose: The focus of this work was given on the relative stopping power (RSP) using the water equivalent thickness (WET) validation on tissue substitutes and real pig organs, as well as a dosimetric comparison of proton treatment plans between single-energy computed tomography (SECT) and dual-energy computed tomography (DECT)-based dose calculations. **Materials and Methods:** The CT calibration curve of SECT and DECT data was generated using the stoichiometric calibration method. WET measurement was performed for RSP validation using a Giraffe dosimeter (IBA dosimetry) in various substitute tissues (Gammex) and real pig tissues. The thorax (008A, CIRS) and head (731-HN, CIRS) phantoms were used to generate proton plans. The dosimetric evaluations of SECT and DECT-based plans were performed using the gamma analysis with 1%/1 mm and the dose–volume histograms (DVHs) comparison. **Results:** For RSP validation of substitute tissues, the largest percent WET difference between measurement and calculation was observed up to 17.9% (4 mm) in lung tissue, using SECT based. In real pig tissues, the average WET difference was 2.3% ± 2.1% and 2.5% ± 2.3% for SECT and DECT, respectively. The average gamma passed of about 92.1% for the lung and 96.8% for the head regions was reported. For the lung region, the DVH of the target dose was observed with a higher predicted dose in SECT than in DECT, while results in the head region were in good agreement for both SECT and DECT. **Conclusion:** The performed dosimetric comparison indicates the dose differences between SECT and DECT. The impact of the CT calibration curve is more pronounced for the thorax region.

Keywords: Dual-energy computed tomography, proton therapy, single-energy computed tomography, stoichiometric method

Received on: 02-03-2023 **Review completed on:** 11-07-2023 **Accepted on:** 14-07-2023 **Published on:** 18-09-2023

Introduction

Proton therapy offers a clinical advantage over photon therapy due to the Bragg peak behavior that can deliver high and escalated doses to the tumor when reducing the dose to surrounding normal tissues.[1-3] The human body consists of tissues with different physical properties and material compositions related to tissue inhomogeneity. The dose calculation and optimization in a patient are affected by tissue inhomogeneity, so computed tomography (CT) images are used and implemented in the treatment planning system (TPS) for accounting for tissue inhomogeneity. In proton TPS, the CT calibration curve requires the relationship between CT number and relative stopping power (RSP). RSP is the proton ranges calculated from proton stopping powers relative to that in water and needed for a treatment plan. The proton range uncertainties depend on the CT calibration curve and can induce inaccurate dose calculation in the TPS.[4-6]

Access this article online

Quick Response Code:

Website: www.jmp.org.in

DOI: 10.4103/jmp.jmp_27_23

Address for correspondence: Dr. Taweap Sanghangthum, Department of Radiology, Faculty of Medicine, Chulalongkorn University, Bangkok, Thailand.
Her Royal Highness Princess Maha Chakri Sirindhorn Proton Center, Bangkok, Thailand.
Department of Radiology, Division of Radiation Oncology, Faculty of Medicine, Chulalongkorn University, Bangkok, Thailand.
E-mail: mairt34@yahoo.com

How to cite this article: Chirdchid T, Ruangchan S, Sanghangthum T. Dosimetric comparison between single-energy computed tomography and dual-energy computed tomography relative to stopping power estimation in proton therapy. J Med Phys 2023;48:292-7.

There are several methods to create the CT calibration curve (Hounsfield unit [HU]-RSP) in proton therapy such as the stoichiometric calibration method. This method was proposed by Schneider *et al*.,[4] and it is the most common method for generating the CT number from single-energy CT (SECT) images to the RSP. However, the range uncertainty from the stoichiometric approach in SECT still exists. Using the dual-energy CT (DECT) is mostly done widely, but only in the research fields and it is limited to implementation in commercial TPS, due to complicated approaches and required more image data to generate the HU-RSP calibration curve. Proton-CT is the ideal method and can directly obtain the RSP distribution inside the patient from proton energy loss. Therefore, proton CT images solve the range errors associated with the X-ray CT-HU. However, it is still under development and inappropriate to use with the current clinical proton TPS.[5]

In human tissues, they may have the same CT number, but RSP may show a difference. The human tissue composition variations can also cause large RSP estimation errors based on SECT since it cannot characterize some tissues with similar CT numbers. DECT is well known for tissue characterization by scanning material at two different energy spectra.[7] The different attenuation of material at two energy levels can reduce RSP estimation errors which is possible to improve the accuracy of patient dose calculation in proton TPS.[4,5,7,8]

In this study, DECT images are the DECT pseudo-monoenergetic CT dataset. The DECT-based still has challenges such as cannot be applied to the commercial TPS and the complicated methods to predict the RSP. Thus, this work aimed to demonstrate the procedure of generating HU-RSP calibration curves following the stoichiometric calibration method, complement existing approaches of the DECT calibration curve in proton therapy, and implement this DECT images in commercial TPS for proton dose calculation.

More specifically, the investigation of the differences of the RSP using water equivalent thickness (WET) comparison in known material compositions (electron density plugs and pig organs) and the difference in dose distribution representing the clinical proton treatment plan in the thorax and head regions for DECT and SECT-based dose calculation is presented and discussed.

Materials and Methods

Proton therapy center

All measurements were carried out at Her Royal Highness Princess Mahachakri Sirindhorn Proton Center (HPSP), King Chulalongkorn Memorial Hospital, Bangkok, Thailand. HPSP center is a single room equipped with 360-degree gantry and pencil beam scanning technique. The available clinical energies for proton ranges are 70–220 MeV which translates into ranges in the water of 40-305 mm and the lateral spot size (sigma) of 6.5 mm for the lowest proton energy (70 MeV) and 3 mm for the highest energy (220 MeV). The accelerator and nozzle design allow for a maximum field size of 30 cm × 40 cm at the isocenter.

Computed tomography calibration curve creation from single-energy computed tomography and dual-energy computed tomography images

The electron density phantom (062M, CIRS Inc., VA, USA) was scanned to access the HU values using GE Healthcare Revolution CT with single energy of 120 kVp and dual-energy of 80/140 kVp. The virtual monoenergetic CT images were generated from DECT images at 70 keV.

The measured HU of electron density phantom from both SECT and DECT data were used to calculate the linear attenuation coefficient of the CT scanner using

$$HU_{measured} + 1000 = 1000\, x\, \mu_i^{rel} = A\left(\rho_{e_i}^{rel} \tilde{Z}_i^{3.62}\right) + B(\rho_{e_i}^{rel} \hat{Z}_i^{1.86}) + C(\rho_{e_i}^{rel})$$

where A, B, and C are constant parameters contributing to the linear attenuation coefficient from photoelectric effect, coherent scattering, and Compton scattering. These constant coefficients are obtained by linear regression.[6]

The μ_i^{rel} and $\rho_{e_i}^{rel}$ are linear attenuation coefficient and electron density relative to water, respectively. The $\tilde{z}_i$ and $\hat{z}_i$ are effective atomic numbers defined using

$$\tilde{Z}_i = \left[\Sigma_j \lambda_j Z_j^{3.62} \right]^{1/3.62}$$

$$\hat{Z}_i = \left[\Sigma_j \lambda_j Z_j^{1.86} \right]^{1/1.86}$$

where $\lambda_j = \frac{W_j Z_j}{A_j} / \Sigma_j \frac{W_j Z_j}{A_j}$, W_j, Z_j and A_j are mass fraction, atomic number, and mass number of element *j* in the composite material *i*, respectively.

The linear attenuation coefficients were used to calculate HU values for CIRS and human tissues which are known for densities and elemental compositions from ICRU Reports of 44 and 46.[9,10]

The proton CT calibration curve requires the relationship of HU values and RSP for dose calculation. The RSP values of CIRS and human tissues can be calculated using the Bethe–Bloch equation[4] which can be approximated by

$$RSP = \rho_e \; ln\left[\frac{2m_e c^2 \beta^2}{I_m(1-\beta^2)} - \beta^2\right] / ln\left[\frac{2m_e c^2 \beta^2}{I_{water}(1-\beta^2)} - \beta^2\right]$$

where $m_e c^2$ is electron rest mass-energy. β is the speed of proton relative to the speed of light. I_m and I_w are the mean excitation energy of tissue and water, respectively.

To generate stoichiometric calibration curve, the HUs were plotted against with RSPs of human tissues and linearly fitted using linear regression within three tissue groups, including bone-like, soft tissues-like, and adipose-like tissues [Figure 1]. CT calibration curves based on DECT and SECT data were

implemented in the Eclipse TPS (TPS V15.06, Varian Medical Systems, Palo Alto, CA, USA).

The relative stopping power validation

The RSP was validated by comparing the WET between TPS and the measurement in various plugs (70 mm thick) of material substitute tissue (model 467, Gammex Inc., WI, USA), Table 1, and real pig organs. In pig organs, the WET measurements were performed in fat, leg, heart, kidney, liver, lung (deflated), muscle, ribs, and mixed tissues of the pig's head. The WET values were acquired from the measurement of the integral depth dose (IDD) using the Giraffe dosimeter (IBA Dosimetry, Schwarzenbruck, Germany) at 220 MeV proton beams as shown in Figure 2a and b. The WET values were obtained by

$$WET = R_{80,air} - R_{80,material}$$

where $R_{80,air}$ and $R_{80,material}$ are the difference of the proton range at 80% dose behind the distal falloff between without material (air) and with material measurements. In addition, the percentage of WET difference was evaluated using

$$\%\ WET\ difference = \frac{|WET_{TPS} - WET_{measured}|}{WET_{measured}} \times 100$$

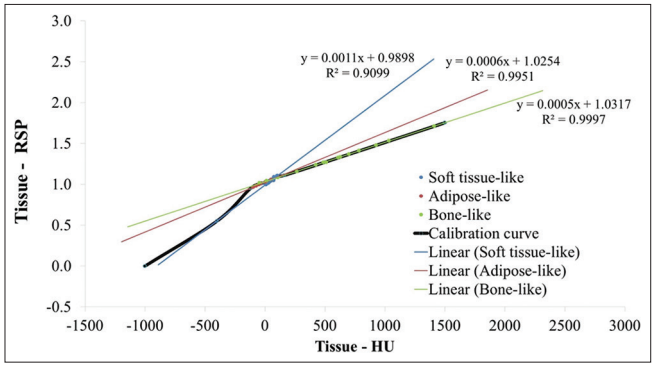

Figure 1: The approach to generating the computed tomography (CT) calibration curve by fitting the linear regression based on 3 groups of human tissues: Soft tissue-like, adipose-like, and bone-like. Data were acquired from the stoichiometric method on dual-energy CT images. RSP: Relative stopping power, HU: Hounsfield unit

The clinical treatment plan validation based on dual-energy computed tomography and single-energy computed tomography calibration curves

The thorax phantom (Model 008A, CIRS Inc., VA, USA) and head phantom (Model 731-HN, ICRS Inc., VA, USA) were selected to represent the clinical scenario in thorax and head regions. Both phantoms were scanned with the DECT and SECT approaches. CT images were imported into the Eclipse TPS and applied the CT calibration curves for each CT data [Figure 2c and d].

To conduct the clinical plan validation, the target was delineated in the thorax and head regions for both DECT and SECT images with different CTV sizes and location. Ten treatment plans were generated (5 for thorax and 5 for head) with the intensity-modulated proton therapy (IMPT) treatment plans, 2 $Gy_{(RBE)}$ prescribed dose, and nonrobustness optimization on SECT data. Once the target is optimized, subsequently, the plans were copied and recalculated based on DECT images. The dose

Table 1: The water equivalent thickness differences between treatment planning system (single-energy computed tomography and dual-energy computed tomography) and measurement in Gammex plugs

Gammex plugs	R_{80} (mm)	$WET_{measured}$ (mm)	WET_{TPS} (mm)		Difference (mm)		Difference (%)		Difference (%)
			SECT	DECT	SECT	DECT	SECT	DECT	SECT-DECT
Soft-tissue									
Solid water	233.0	72.4	72.2	73.0	−0.2	0.6	−0.3	0.8	−0.5
Breast	235.0	70.4	69.9	70.8	−0.5	0.4	−0.7	0.6	0.1
Liver	228.2	77.2	76.4	77.2	−0.8	0.0	−1.0	0.0	1.0
Adipose	237.4	68.0	67.4	68.4	−0.6	0.4	−0.9	0.6	0.3
Brain	228.7	76.7	72.3	73.6	−4.4	−3.1	−5.7	−4.0	1.7
Average±SD					1.3±1.7	0.9±1.2	1.7±2.3	1.2±1.6	0.7±0.6
Bone									
Bone (CB2 30%)	214.7	90.7	88.6	90.6	−2.1	−0.1	−2.3	−0.1	−2.2
Bone (CB2 50%)	203.5	101.9	102.0	105.0	0.1	3.1	0.1	3.0	−2.9
Bone (B200)	225.7	79.7	80.4	82.1	0.7	2.4	0.9	3.0	−2.1
Cortical bone	190.2	115.2	117.8	121.4	2.6	6.2	2.3	5.4	−3.1
Inner bone	226.5	78.9	80.0	82.0	1.1	3.1	1.4	3.9	−2.5
Average±SD					1.3±1.0	3.0±2.2	1.4±0.9	3.1±1.9	2.6±0.4
Lung									
Lung 300	283.1	22.3	18.3	19.0	−4.0	−3.3	−17.9	−14.8	−3.1
Lung 450	273.1	32.3	28.2	29.0	−4.1	−3.3	−12.7	−10.2	−2.5
Average±SD					4.1±0.1	3.3±0.0	15.3±3.7	12.5±3.2	2.8±0.3

CT: Computed tomography, WET: Water equivalent thickness, TPS: Treatment planning system, SECT: Single-energy CT, DECT: Dual-energy CT, SD: Standard deviation

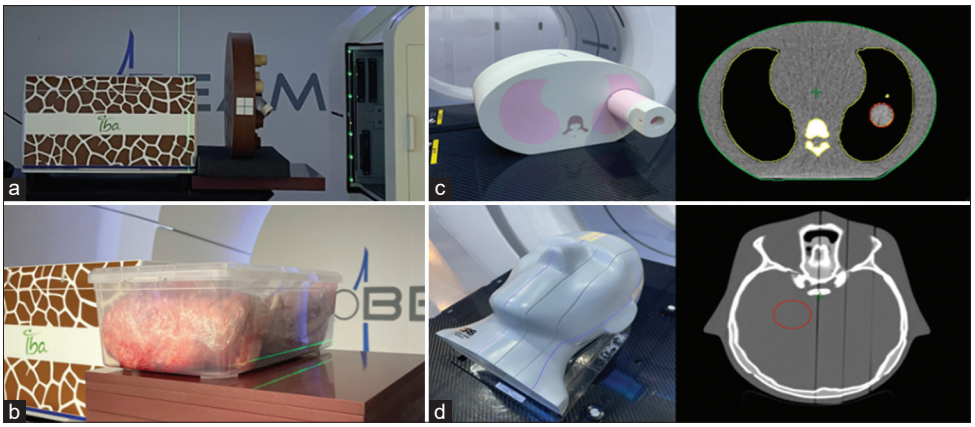

Figure 2: (a and b) The water equivalent thickness measurements in Gammex plugs and pig organs using Giraffe dosimeter (IBA Dosimetry), (c and d) The thorax and head phantoms together with their computed tomography images in the treatment planning system

distributions between the DECT and SECT were compared using the 1%/1 mm gamma analysis as well as the target dose–volume histograms (DVHs) were taken for evaluation.

Results

Dual-energy computed tomography and single-energy computed tomography calibration curves

The CT calibration curve was created by plotting the calculated HU against the RSP of reference tissues. The HU of reference tissues were calculated using the stoichiometric calibration method and their RSP was calculated from the Bethe–Bloch equation. The CT calibration curve-based SECT and DECT were linearly fitted using linear regression for three tissue groups: bone-like, soft tissue-like, and adipose-like tissues. Figure 3 shows the CT calibration curves of both DECT and SECT data.

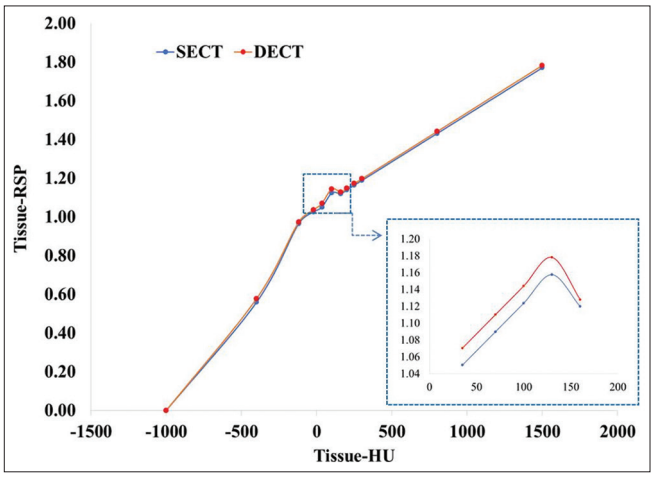

Figure 3: The computed tomography (CT) calibration curve-based single-energy CT (blue line) and dual-energy CT (red line). RSP: Relative stopping power, SECT: Single-energy computed tomography, DECT: Dual-energy computed tomography, HU: Hounsfield unit

The relative stopping power validation

The WET measurement was performed for RSP validation at 220 MeV proton beams. The R_{80} without material insertion (open beam) was 305.4 mm. In Gammex plugs, the R_{80} of each plug and the WET difference values between measurement and calculation are shown in Table 1. For SECT based, the average and standard deviation of percent WET difference were 1.7% ± 2.3% for the soft-tissues group, 1.4% ± 0.9% for the bone group, and 15.3% ± 3.7% for lung group. The average and standard deviation of percent WET difference for DECT based were 1.2% ± 1.6% for the soft-tissues group, 3.1% ± 1.9% for the bone group, and 12.5% ± 3.2% for the lung group. The maximum WET difference was found in lung 300 for SECT based with the maximum WET deviation of − 17.9% (-4.0 mm).

For real pig organs, the maximum percent WET difference was observed in lung tissues for the SECT based with a deviation of − 5.8% (−5.0 mm) and for the DECT based with the difference of 7.5% (7.0 mm) in pig ribs. The average percent WET difference was 3.0% ± 2.3% and 3.2% ± 2.4% for the SECT and DECT-based curves, respectively. The average percent WET differences of mixed tissues (pig head) for the SECT and DECT based were 0.9% ± 0.3% and 0.9% ± 1.0%, respectively. The R_{80}, measured WET, calculated WET from the TPS and WET differences of pig tissues are shown in Table 2. The average percent WET differences for all tissues were 2.3% ± 2.1% for SECT and 2.5% ± 2.3% for DECT. The WET difference between SECT and DECT was compared using Wilcoxon signed-rank test with no significant difference ($P > 0.05$).

The clinical treatment plan validation based on dual-energy computed tomography and single-energy computed tomography calibration curves

The percent gamma passing rate of 10 IMPT plans in the thorax and head phantoms is shown in Table 3. The average and standard deviation of gamma passing rate of SECT and DECT were 92.1% ± 4.4% for the thorax and 96.8% ± 1.8% for the head region. Figure 4 presents the dose distribution of DECT and SECT-based dose calculation, gamma distribution, and the DVHs of the target volume in the thorax phantom.

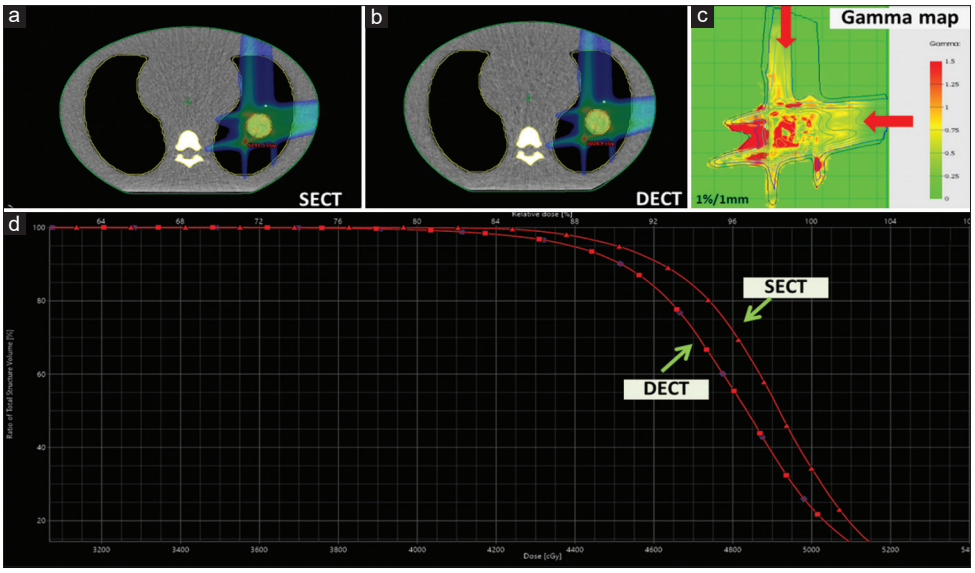

Figure 4: An example of the dose calculation in the thorax and the dosimetric comparison between single-energy computed tomography (SECT) and dual-energy computed tomography (DECT)-based dose calculation. (a and b) The dose distribution in SECT and DECT images. (c) The dosimetric comparison using the gamma analysis for 1%/1mm; red arrows indicate the proton beam direction. (d) The dose–volume histograms comparison of the target dose. SECT: Single-energy computed tomography, DECT: Dual-energy computed tomography

Table 2: The water equivalent thickness differences between treatment planning system (single-energy CT and dual-energy CT) and measurement in real pig organs

Tissues	R_{80} (mm)	$WET_{measured}$ (mm)	WET_{TPS} (mm)		Difference (mm)		Difference (%)		Difference (%)
			SECT	DECT	SECT	DECT	SECT	DECT	SECT-DECT
Individual organ									
Fat	252.3	53.0	55.1	56.4	2.1	3.4	3.9	6.3	−2.4
Heart	219.2	86.2	81.9	84.1	−4.3	−2.1	−5.0	−2.4	2.6
Liver	241.5	63.9	64.0	65.1	0.1	1.2	0.2	1.9	−1.7
Kidney	227.3	78.1	78.7	80.0	0.6	1.9	0.8	2.4	−1.6
Leg	242.9	62.4	60.8	62.1	−1.6	−0.3	−2.6	−0.6	2.0
Rib	211.6	93.8	98.6	100.8	4.8	7.0	5.1	7.5	−2.4
Muscle	238.6	66.7	66.5	67.6	−0.2	0.9	−0.4	1.3	−0.9
Lung (deflated)	218.6	86.7	81.7	83.7	−5.0	−3.0	−5.8	−3.5	2.3
Average±SD					2.3±2.1	2.5±2.1	3.0±2.3	3.2±2.4	2.0±0.6
Pig head (mixed tissues)									
Head 1*	1376.0	167.8	169.8	171.8	2.0	4.0	1.2	2.4	−1.2
Head 2*	1634.0	142.0	142.6	143.2	0.6	1.2	0.4	0.9	−0.5
Mouth	1768.5	128.5	127.5	128.5	−1.0	0.0	−0.8	0.0	0.8
Nose	1977.5	107.6	106.5	108.2	−1.1	0.6	−1.1	0.5	0.6
Average±SD					1.2±0.6	1.5±1.8	0.9±0.3	0.9±1.0	0.8±0.3

*The positions of WET measurement in head 1 and head 2 were 5 cm and 4 cm away from the isocenter. CT: Computed tomography, WET: Water equivalent thickness, TPS: Treatment planning system, SECT: Single-energy CT, DECT: Dual-energy CT, SD: Standard deviation

Discussion

Besides the limitation of DECT implementation in the clinical TPS, this research studied the comparison of dosimetric differences between using SECT and DECT for RSP estimation in proton therapy. The CT calibration curves were created based on the stoichiometric calibration method from SECT images and virtual monoenergetic images (DECT).

The RSP validation was firstly performed in Gammex phantom. The average percent WET difference value was within 2% for the soft tissues, 3% for the bone, and 16% for lung plugs. In lung tissue, the percent WET difference of SECT based was higher than DECT. The results are in line with the studies of Kassaee *et al*.[8] and Hudobivnik *et al*.,[11] showing the maximum RSP difference between the predicted RSP-based SECT and DECT in lung tissue. Large uncertainties in WET of lung phantom might cause by the natural porous structures of lung plugs. The inhomogeneity of lung structure relates to the partial volume effect which may lead to the inaccurate CT number and RSP estimation.[11]

Table 3: The percent gamma passing rate of intensity-modulated proton therapy treatment plans in thorax and head regions

IMPT plans	Percent gamma passing rate	
	Thorax	Head
Plan number 1	88.5	99.3
Plan number 2	92.1	95.3
Plan number 3	99.6	95.8
Plan number 4	91.2	98.3
Plan number 5	89.3	95.4
Average±SD	92.1±4.4	96.8±1.8

SD: Standard deviation, IMPT: Intensity-modulated proton therapy

In pig organs, DECT data were observed for maximum percent WET difference only in rib tissues, due to the RSP sensitivity to dense bone composition variations and beam hardening effect on CT images. Besides that, the virtual monoenergetic CT images (DECT) generated from a rapid kVp switching scanner are more influenced by the beam hardening effect in bone tissues compared to SECT images. The beam hardening effect relates to the inaccurate CT number and RSP estimation errors. Park *et al*.[12] and Ohira *et al*.[13] suggested generating virtual monoenergetic CT images (DECT) with higher energy due to the reduction of beam hardening effect from the Compton effect characteristic. In addition, the positioning of pig organs in acquiring CT scanned and WET measurements is one of the most challenging task, since the position of the pig organs placed in the container could have a possibility to move during the transportation between CT and proton treatment rooms. However, the average WET difference based on two curves was well presented within the clinical range uncertainty acceptable of 3.5%.[6,12]

Concerning the dosimetric evaluation in the clinical IMPT plan, the dosimetric evaluations were performed using the 1%/1 mm gamma analysis in the thorax and head regions. The dosimetric difference between SECT and DECT-based curves showed more impact in the lung region compared to the head region [Figure 4c], due to the uncertainties in the predicted theoretical CT numbers of the lung substitutes and the RSP calculation on the various atomic composition of human lung tissues (section 2.2). Range uncertainties are induced by the errors in estimated RSPs from the conversion of CT-HU and are more pronounced in low-density tissues which could impact the dose deviation between SECT and DECT. The DVH of the target dose was observed with a higher predicted dose in SECT than in DECT [Figure 4d], whereas the results in the head region were in good agreement for both images. These results are in line with with Kassaee *et al*.[8] and Wohlfahrt *et al*.[14] who reported no dose distribution changes in head treatment plans.

Conclusion

The stoichiometric method for generating the HU-RSP calibration curve of SECT and DECT based-dose calculation implemented in the commercial TPS indicates the dose differences. The DECT-based curve has the potential to improve the accuracy of RSP estimation. This Stoichiometric method for DECT could be taken for dose calculation and treatment plan evaluation in commercial TPS. The impact of the CT calibration curve is more pronounced for the thorax region, whereas the results for head treatment plans show a more comparable dose distribution.

Acknowledgments

The HRSP Proton Center at King Chulalongkorn Memorial Hospital providing materials and proton beam times for the experimental measurements is gratefully acknowledged.

Financial support and sponsorship

Nil.

Conflicts of interest

There are no conflicts of interest.

References

1. Schulz-Ertner D, Tsujii H. Particle radiation therapy using proton and heavier ion beams. J Clin Oncol 2007;25:953-64.
2. Semwal M. Khan's the physics of radiation therapy. J Med Phys 2020;45:134-5.
3. Jäkel O. Physical advantages of particles: protons and light ions. Br J Radiol. 2020;93(1107):20190428. doi: 10.1259/bjr.20190428.
4. Schneider U, Pedroni E, Lomax A. The calibration of CT Hounsfield units for radiotherapy treatment planning. Phys Med Biol 1996;41:111-24.
5. Schulte RW, Penfold SN. Proton CT for improved stopping power determination in proton therapy, invited. Trans Am Nucl Soc 2012;106:55-8.
6. Ainsley CG, Yeager CM. Practical considerations in the calibration of CT scanners for proton therapy. J Appl Clin Med Phys 2014;15:4721.
7. Goo HW, Goo JM. Dual-energy CT: New Horizon in medical imaging. Korean J Radiol 2017;18:555-69.
8. Kassaee A, Cheng C, Yin L, Zou W, Li T, Lin A, *et al.* Dual-energy computed tomography proton-dose calculation with scripting and modified Hounsfield units. Int J Part Ther 2021;8:62-72.
9. ICRU. Tissue Substitutes in Radiation Dosimetry and Measurement, in – Ternational Commission on Radiation Units and Measurements Report 44; 1989.
10. ICRU. Photon, Electron, Proton, and Neutron Interaction Data for Body Tissues, International Commission on Radiation Units and Measurements Report 46; 1992.
11. Hudobivnik N, Schwarz F, Johnson T, Agolli L, Dedes G, Tessonnier T, *et al.* Comparison of proton therapy treatment planning for head tumors with a pencil beam algorithm on dual and single energy CT images. Med Phys 2016;43:495.
12. Park YK, Sharp GC, Phillips J, Winey BA. Proton dose calculation on scatter-corrected CBCT image: Feasibility study for adaptive proton therapy. Med Phys 2015;42:4449-59.
13. Ohira S, Imai Y, Koike Y, Ono S, Ueda Y, Miyazaki M, *et al.* Evaluation of stopping power ratio calculation using dual-energy computed tomography with fast kilovoltage switching for treatment planning of particle therapy. *In Vivo* 2022;36:103-10.
14. Wohlfahrt P, Möhler C, Hietschold V, Menkel S, Greilich S, Krause M, *et al.* Clinical implementation of dual-energy CT for proton treatment planning on pseudo-monoenergetic CT scans. Int J Radiat Oncol Biol Phys 2017;97:427-34.